Chlorine NQR Spin-Lattice Relaxation and Electron Spin Dynamics in Paramagnetic $[Co(H_2O)_6][PtCl_6]$

Motohiro Mizuno, Tetsuo Asaji, Atsushi Tachikawa, and the late Daiyu Nakamura

Department of Chemistry, Faculty of Science, Nagoya University, Nagoya, Japan

Z. Naturforsch. **46a**, 1103–1107 (1991); received September 17, 1991

Chlorine NQR spin-lattice relaxation times T_{1Q} were determined for $[Co(H_2O)_6][PtCl_6]$ at 4.2–400 K. Above ca. 350 K, T_{1Q} decreased rapidly showing the onset of a reorientation of $[PtCl_6]^{2-}$. The activation energy E_a of this reorientation was determined as 125 ± 15 kJ mol^{-1}. With decreasing temperature, T_{1Q} showed a maximum at ca. 250 K. Below ca. 200 K, T_{1Q} is governed by the magnetic dipolar interaction between chlorines and paramagnetic Co^{2+} ions and is inversely proportional to the electron spin correlation time τ_e of Co^{2+}. τ_e is shown to be determined by the electron spin-lattice relaxation time T_{1e} and the temperature independent correlation time τ_s for the spin-exchange between neighbouring ions above and below ca. 50 K, respectively. The temperature dependence of T_{1e} is explained by assuming the Orbach process with an energy gap Δ/k of 530 ± 20 K as $T_{1e} = 5 \times 10^{-14} \exp(530/T)$ s. τ_s was estimated to be 0.9×10^{-10} s.

The temperature dependence of the ESR linewidth of Mn^{2+} impurities in single crystal was also measured, intending to study Co^{2+} spin dynamics. The limit of the ESR method is discussed by comparing the obtained results with those of the NQR method.

Key words: Spin-lattice relaxation, NQR, ESR, Reorientation, Orbach process.

Introduction

The spin-lattice relaxation time T_{1e} of Co^{2+} is very short at normal temperatures in an octahedral crystal field [1]. Above 77 K, therefore, even a detection of ESR signals is usually impossible due to the life-time broadening. To investigate such a fast spin dynamics of Co^{2+}, ESR of paramagnetic impurity ions doped in the host cobalt salts can be used; the impurity linewidth can reflect the host T_{1e}, since the linewidth is determined by the host-impurity interaction averaged by the "host spin-lattice relaxation narrowing" mechanism [2–7]. In this method, however, it is not easy to estimate the linewidth in the absence of the narrowing mechanism, because both dipolar and exchange interactions between dissimilar ions, where the latter are generally unknown, contribute to the line broadening. Hence, T_{1e} calculated by use of only the dipolar width is just longer limit of the host spin-lattice relaxation time.

Nuclear spin-lattice relaxation times can also give information on the electron spin dynamics in paramagnetic salts [8–10]. For the localized spin system it is easy to estimate the dipolar coupling between paramagnetic ions and the resonant nucleus which governs the nuclear relaxation. Therefore spin-lattice relaxation time measurements of an NMR or NQR nucleus are expected to be more reliable for the study of fast paramagnetic spin dynamics. In this paper we report the application of the chlorine NQR method to study the Co^{2+} spin dynamics in $[Co(H_2O)_6][PtCl_6]$. The ESR method of impurity Mn^{2+} ions doped in a $[Co(H_2O)_6][PtCl_6]$ single crystal is also examined for comparison.

The crystal of $[Co(H_2O)_6][PtCl_6]$ belongs to the space group $R\bar{3}$, $a = 7.10$ Å, $\alpha = 96.26°$, $Z = 1$ [11], and its structure is a slightly distorted CsCl structure composed of the octahedral complexes $[Co(H_2O)_6]^{2+}$ and $[PtCl_6]^{2-}$. Both complex ions are located at $\bar{3}$ sites of the crystal lattice although the atomic positions of chlorines and oxygens are not known. In accord with the crystal structure, a single ^{35}Cl NQR frequency has been reported at 4.2–400 K, and no phase transition has been observed [12].

Experimental

Equimolar amounts of $H_2PtCl_6 \cdot 6H_2O$ and $CoCl_2 \cdot 6H_2O$ were dissolved in a small amount of water [12, 13]. The solution was heated on a water bath until

Reprint requests to Dr. T. Asaji, Department of Chemistry, Faculty of Science, Nagoya University, Nagoya 464-01, Japan.

0932-0784 / 91 / 1200-1103 $ 01.30/0. – Please order a reprint rather than making your own copy.

dryness without a smell of HCl. The residual was dissolved in water and was filtered off. $[Co(H_2O)_6][PtCl_6]$ crystals were obtained by slow concentration of the solution in a desiccator by P_2O_5 and NaOH. For the NQR measurements, the polycrystalline sample was sealed in a glass tube with a small amount of He gas. Mn^{2+} doped single crystals of $[Co(H_2O)_6][PtCl_6]$ were prepared from a solution containing a 1/100 molar amount of $[Mn(H_2O)_6][PtCl_6]$, which was synthesized similarly using $MnCl_2 \cdot 4H_2O$.

A homemade pulsed NQR spectrometer was used for the spin-lattice relaxation time T_{1Q} measurements [14, 15]. The $180°-\tau-90°-\tau_e-180°$ pulse sequence was applied, where the spacing time τ was varied while τ_e was set constant (100–500 μs). The error of T_{1Q} measurements is estimated to be ca. ±10%. The sample temperature was controlled with temperature controllers, Ohkura EC-61 and Oxford DTC2, equipped with copper-constantan and gold (0.07% Fe)-chromel thermocouples above and below 77 K, respectively. The temperature was estimated to be accurate within ±1 K.

Mn^{2+} ESR spectra of a Mn^{2+} doped single crystal of $[Co(H_2O)_6][PtCl_6]$ were recorded by use of a JEOL SCXA X-band spectrometer with a TE_{011} cylindrical cavity resonator [16, 17]. From the rotation patterns of the ESR spectra, the [1, 1, 1] axis of the crystal was identified. DPPH was used as a marker of the magnetic field. A copper-constantan thermocouple located close to the crystal but outside of the cavity was used for temperature measurements, the accuracy of which was estimated as ±5 K.

Least-squares fitting calculations to the observed data were performed with a theoretical equation by use of SALS reported by Oyanagi and Nakagawa [18] at Nagoya University Computation Center.

Results and Discussion

Spin-Lattice Relaxation of Chlorine Nuclear Quadrupole Resonance

The ^{35}Cl NQR frequencies determined agreed very well with those reported [12]. They and the spin-lattice relaxation times T_{1Q} of ^{35}Cl and ^{37}Cl are listed in Table 1 for $[Co(H_2O)_6][PtCl_6]$ at several temperatures. Figure 1 shows the temperature dependences of T_{1Q} of ^{35}Cl and ^{37}Cl NQR in $[Co(H_2O)_6][PtCl_6]$. A T_{1Q} maximum was observed at ca. 250 K. The rapid decrease above ca. 350 K can be attributed to the onset of a reorientation of $[PtCl_6]^{2-}$, since $T_{1Q}(^{37}Cl)/T_{1Q}(^{35}Cl)=1$ was obtained [19]. On the other hand, the T_{1Q} decrease on the lower-temperature side can not be explained by the lattice vibrational relaxation process which is usually operative at low temperatures [19]. T_{1Q} showed a constant value of ca. 0.55 ms below ca. 50 K. The ratio $T_{1Q}(^{37}Cl)/T_{1Q}(^{35}Cl)=1.46\pm0.1$ obtained below ca. 200 K suggests that the relaxation process is dominated by the magnetic dipolar interaction between chlorines and paramagnetic Co^{2+} ions, which gives $T_{1Q}(^{37}Cl)/T_{1Q}(^{35}Cl)=[\gamma(^{35}Cl)/\gamma(^{37}Cl)]^2=1.44$ using the square of the ratio of the gyromagnetic ratios γ [19].

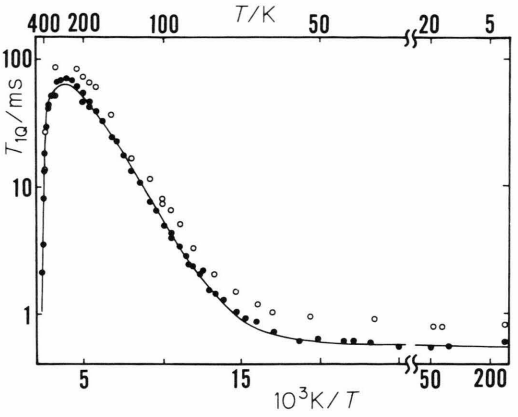

Fig. 1. Temperature dependences of ^{35}Cl (●) and ^{37}Cl (○) NQR spin-lattice relaxation times T_{1Q} in $[Co(H_2O)_6][PtCl_6]$. The solid line shows a best-fitted theoretical curve for ^{35}Cl T_{1Q} using (13).

Table 1. NQR frequencies ν and spin-lattice relaxation times T_{1Q} of ^{35}Cl and ^{37}Cl nuclei in $[Co(H_2O)_6][PtCl_6]$ at several temperatures.

T/K	^{35}Cl ν / MHz	^{37}Cl ν / MHz	^{35}Cl T_{1Q} / ms	^{37}Cl T_{1Q} / ms
4.2	25.827	20.357	0.60	0.82
32.0	25.825	20.356	0.55	0.82
62.5	25.819	20.349	0.84	1.2
75.0	25.816	20.347	1.4	2.0
90.5	25.810	20.342	3.3	4.9
149	25.793	20.328	24	36
298	25.759	20.300	67	88
380	25.736	20.282	29	26
396	25.730	20.279	13	14

The spin-lattice relaxation rate $(T_{1Q}^{-1})_e$ of chlorine ($I=3/2$, gyromagnetic ratio γ) due to the magnetic interaction with paramagnetic Co^{2+} ions (g-value $\tilde{g}$ and fictitious angular momentum $\tilde{J}$) can be written as

$$(T_{1Q}^{-1})_e = 3\left(\tfrac{9}{2}\right)\gamma^2\tilde{g}^2\mu_B^2\left[\tfrac{1}{3}\tilde{J}(\tilde{J}+1)\right](2\tau_e)\Lambda \qquad (1)$$

by assuming a fast isotropic fluctuations of $\tilde{J}$ [20]. Here, μ_B, τ_e, and Δ denote Bohr magneton, the electron spin correlation time of a Co^{2+} ion, and a geometrical factor depend on internuclear vectors between the resonant nucleus and paramagnetic ions. The geometrical factor Δ is given by

$$\Delta = \sum_i \{|F_i^{(1)}|^2 + \tfrac{1}{18}|F_i^{(0)}|^2 + \tfrac{1}{2}|F_i^{(2)}|^2\}, \quad (2)$$

using the spatial parts of the dipolar Hamiltonian

$$|F_i^{(0)}|^2 = (1-3\cos^2\theta_i)^2 r_i^{-6}, \quad (3)$$

$$|F_i^{(1)}|^2 = (\sin^2\theta_i \cos^2\theta_i) r_i^{-6}, \quad (4)$$

$$|F_i^{(2)}|^2 = (\sin^4\theta_i) r_i^{-6}, \quad (5)$$

where r_i is the distance between the resonant nucleus and the i-th paramagnetic ion, and θ_i is the angle between the z axis of the electric field gradients (EFG) tensor at chlorine and the distance vector r_i.

The electron spin correlation time τ_e can be written by the temperature-dependent electron spin-lattice relaxation time T_{1e} and the temperature-independent characteristic time τ_s for the spin flip between neighbouring electrons as [8]

$$\tau_e^{-1} = T_{1e}^{-1} + \tau_s^{-1}. \quad (6)$$

Hence, by assuming the Orbach process [21]:

$$T_{1e} = a \exp(\Delta/kT) \quad (7)$$

for the electron spin-lattice relaxation process in the instantaneous local magnetic field, where Δ denotes the energy difference between the ground and the first-excited states of Co^{2+}, the temperature dependence of T_{1Q} observed below ca. 200 K can be interpreted by (1). Equation (1) can be rewritten as

$$(T_{1Q}^{-1})_e = K\{a^{-1}\exp(-\Delta/kT) + \tau_s^{-1}\}^{-1}, \quad (8)$$

where

$$K = 3(\tfrac{9}{2})\gamma^2\tilde{g}^2\mu_B^2[\tfrac{1}{3}\tilde{J}(\tilde{J}+1)](2\Delta) \quad (9)$$

$$= 9\gamma^2\mu_{eff}^2\Delta, \quad (10)$$

using the effective Bohr magneton $\mu_{eff} = [\tilde{g}^2\mu_B^2\tilde{J}(\tilde{J}+1)]^{1/2}$ for the Co^{2+} ion. In the following calculations we have assumed that $\mu_{eff}^2 = 24\,\mu_B^2$, the value of which was determined for the isomorphous $[Co(H_2O)_6][SiF_6]$ [22], and that $\Delta = 1.63\times10^{44}\,cm^{-6}$, which was estimated from the crystal structure of the isomorphous $[Ni(H_2O)_6][SnCl_6]$ [11, 20].

To explain the T_{1Q}^{-1} values in the whole temperature range, the contributions $(T_{1Q}^{-1})_l$ and $(T_{1Q}^{-1})_r$ from lattice vibrations and a reorientation of the $[PtCl_6]^{2-}$ complex anions, respectively, should be considered. These relaxation contributions can be written as

$$(T_{1Q}^{-1})_l = bT^2 \quad (11)$$

and

$$(T_{1Q}^{-1})_r = c\exp(-E_a/RT), \quad (12)$$

where E_a is the activation energy of the reorientation [19]. Using the formula

$$T_{1Q}^{-1} = (T_{1Q}^{-1})_e + (T_{1Q}^{-1})_l + (T_{1Q}^{-1})_r, \quad (13)$$

least-squares fitting calculations were performed with a, Δ, τ_s, b, c, and E_a as parameters. The best-fit parameters are listed in Table 2.

Table 2. The optimized parameters for the respective contributions to the spin-lattice relaxation rate of ^{35}Cl NQR of $[Co(H_2O)_6][PtCl_6]$ (see text).

Magnetic interaction with paramagnetic Co^{2+} ions	a/s	5×10^{-14}
	(Δ/k)/K	530 ± 20
	τ_s/s	0.9×10^{-10}
Lattice vibrations	$b/s^{-1}K^{-2}$	1×10^{-4}
Reorientation of $[PtCl_6]^{2-}$	c/s^{-1}	2×10^{18}
	E_a/kJ mol^{-1}	125 ± 15

The electron spin-lattice relaxation time T_{1e} and the temperature-independent time τ_s are given by

$$T_{1e} = 5\times10^{-14}\exp(530/T)\,s, \quad (14)$$

$$\tau_s = 0.9\times10^{-10}\,s. \quad (15)$$

The energy difference $\Delta/k = 530\pm20$ K ($370\pm15\,cm^{-1}$) obtained for the ground and the first-excited states of the Co^{2+} compares quite well with the experimentally reported values of several compounds [8, 10, 23, 24]. Theoretically, Δ equals $(3/2)\tilde{\lambda}$ for the Co^{2+} ions in a cubic crystal field, where $\tilde{\lambda}$ is the effective spin-orbit parameter of Co^{2+} [25].

ESR Spectra of Mn^{2+} in $[Co(H_2O)_6][PtCl_6]$

The observed ESR spectra of Mn^{2+} ($S=I=5/2$) consist of 30 lines, as shown in Fig. 2, and are indicating the existence of a single type of $[Mn(H_2O)_6]^{2+}$ magnetic complexes in the trigonal ($R\bar{3}$) crystal of $[Co(H_2O)_6][PtCl_6]$. The spectra could be described by an effective spin-Hamiltonian appropriate for trigonal crystal field symmetry:

$$\mathcal{H} = g_{\parallel}\mu_B H_z S_z + g_{\perp}\mu_B(H_x S_x + H_y S_y) + D[S_z^2 - \tfrac{1}{3}S(S+1)] + A_{\parallel}S_z I_z + A_{\perp}(S_x I_x + S_y I_y) + \frac{a}{6}[S_x^4 + S_y^4 + S_z^4 - \tfrac{1}{5}S(S+1)(3S^2+3S-1)], \quad (16)$$

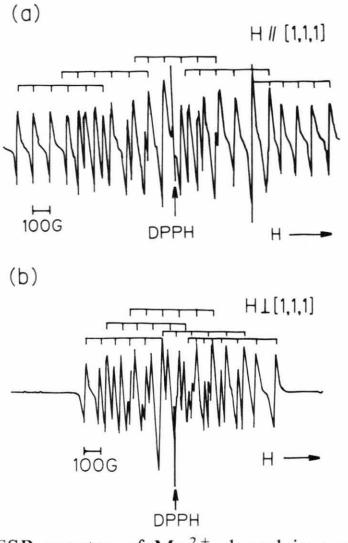

Fig. 2. ESR spectra of Mn^{2+} doped in a single crystal of $[Co(H_2O)_6][PtCl_6]$ at room temperature. The magnetic field is parallel and perpendicular to the [1, 1, 1] axis of the crystal, respectively, for (a) and (b).

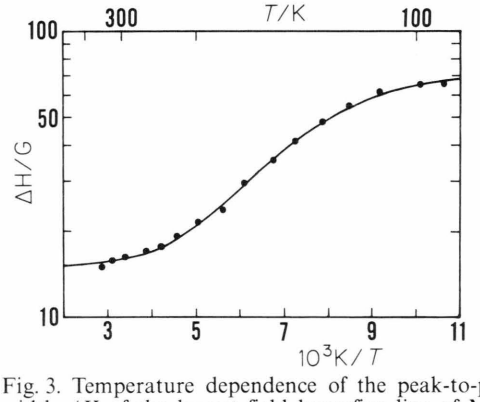

Fig. 3. Temperature dependence of the peak-to-peak linewidth ΔH of the lowest field hyperfine line of Mn^{2+} in a single crystal of $[Co(H_2O)_6][PtCl_6]$. The magnetic field is parallel to the [1, 1, 1] axis of the crystal. The solid line shows a best-fitted theoretical curve by use of (21) in the text.

where μ_B is the Bohr magneton, $H=(H_x, H_y, H_z)$ the external magnetic field, $S=(S_x, S_y, S_z)$ the electron spin operator, and the others have their usual meaning [4, 5, 26–28]. The spectra described by (16) are invariant with respect to the rotation of the field about the [1, 1, 1] axis of the crystal, and maximum spread of the spectrum is observed when the magnetic field is parallel to the [1, 1, 1] axis [5]. The spin-Hamiltonian parameters determined at room temperature are $g_{\parallel}=g_{\perp}=2.00$, $|D|=168$ G, $|A_{\parallel}|=97$ G, $|A_{\perp}|=96$ G, and $|a|=8$ G, in the unit of magnetic field for the electron ($1\,G=10^{-4}$ T).

Modulation Narrowing of Mn^{2+} ESR Spectra due to Co^{2+} Spin-Lattice Relaxation

The peak-to-peak linewidth ΔH of the lowest field hyperfine line was measured as a function of temperature when the magnetic field was applied along the [1, 1, 1] axis. ΔH decreases from 65 G at ca. 90 K to 15 G at ca. 300 K with increasing temperature as shown in Figure 3. The square of the linewidth can be written approximately as

$$(\Delta H)^2=(\Delta H_{\text{Mn-Co}})^2+(\Delta H_{\text{Mn-H}})^2, \tag{17}$$

provided that $\Delta H_{\text{Mn-Co}}$ and $\Delta H_{\text{Mn-H}}$ result from the two independent broadening mechanism, that is, the magnetic interaction between Mn^{2+} and Co^{2+} ions and the magnetic dipolar interaction between Mn^{2+} and ^1H of water molecule, respectively [2]. Owing to the modulation narrowing due to the rapid electron spin correlation time τ_e of Co^{2+}, the $\Delta H_{\text{Mn-Co}}$ is given by [2]

$$\Delta H_{\text{Mn-Co}}=\frac{2(\Delta H^0_{\text{Mn-Co}})^2}{H_{\text{mod}}}. \tag{18}$$

Here, $\Delta H^0_{\text{Mn-Co}}$ denotes the linewidth in the absence of the modulation, and the modulation field H_{mod} is defined by use of τ_e and the g-value $\tilde{g}$ of Co^{2+}:

$$\tilde{g}\,\mu_B H_{\text{mod}}=h/\tau_e. \tag{19}$$

From (17)–(19) we have

$$(\Delta H)^2=\left[\frac{2\tilde{g}\,\mu_B}{h}(\Delta H^0_{\text{Mn-Co}})^2\,\tau_e\right]^2+(\Delta H_{\text{Mn-H}})^2. \tag{20}$$

Adopting the relations (6) and (7) for τ_e and T_{1e}, respectively, (20) becomes

$$(\Delta H)^2=A\,[\exp(-\Delta/kT)+B]^{-2}+(\Delta H_{\text{Mn-H}})^2, \tag{21}$$

where

$$A=\left[\frac{2a\tilde{g}\,\mu_B}{h}(\Delta H^0_{\text{Mn-Co}})^2\right]^2, \tag{22}$$

$$B=a\,\tau_s^{-1}. \tag{23}$$

Least-squares fitting calculations by use of (21) resulted in $A=0.3$ G^2, $B=8\times10^{-3}$, $\Delta/k=680\pm150$ K, $\Delta H_{\text{Mn-H}}=15\pm2$ G for the observed temperature dependence of ΔH shown in Figure 3. The obtained value of $\Delta H_{\text{Mn-H}}$ is quite reasonable compared with the estimated values of 10–15 G [29]. The energy gap parameter Δ agrees fairly well with that ($\Delta/k=530$ K) obtained from the ^{35}Cl T_{1Q} analysis. These results suggest that the ESR linewidth analysis of impurity paramagnetic ions can be applied to investigate the

fast electron spin dynamics of host paramagnetic ions. However, to obtain the absolute value of the Co^{2+} spin-lattice relaxation time T_{1e}, it is necessary to know the value of $\Delta H^0_{Mn\text{-}Co}$, which is very difficult to estimate because the additional contribution from the exchange interaction between dissimilar ions is superimposed on the dipolar width [2].

The dipolar width due to the Mn-Co interaction can be evaluated from the second moment M_2 for dipolar broadening. Taking into account of only the adiabatic part of the dipolar Hamiltonian between dissimilar ions (Mn-Co), M_2 of Mn^{2+} ESR line is given by [30]

$$M_2 = (\tfrac{1}{3})\,\mu_{eff}^2 \sum_k r_{jk}^{-6}(3\cos^2\theta_{jk} - 1)^2, \tag{24}$$

where μ_{eff} is the effective Bohr magneton of the Co^{2+} ion and θ_{jk} is the angle between the magnetic field direction and the interionic vector r_{jk} connecting the j-th Mn^{2+} to the k-th Co^{2+}. For a Gaussian lineshape, the purely dipolar width $(\Delta H^0_{Mn\text{-}Co})_{dip}$ is estimated by

$$(\Delta H^0_{Mn\text{-}Co})^2_{dip} \approx 4\,(\tfrac{10}{3})\,M_2\,. \tag{25}$$

Here, the relation between the peak-to-peak width and the second moment was employed, and the so-called "10/3 effect" was taken into account in order to include the second moment contribution from the nonadiabatic term of the dipolar Hamiltonian [31]. Based on the crystal structure $R\bar{3}$, $a = 7.10$ Å, $\alpha = 96.26°$ [11], and using $\mu^2_{eff}(\parallel [1,1,1]) = 33\,\mu_B^2$ [32] for $[Co(H_2O)_6][PtCl_6]$, $(\Delta H^0_{Mn\text{-}Co})^2_{dip}$ was calculated to be $27 \times 10^4\,G^2$ when the external field is parallel to the [1, 1, 1] axis.

Putting $(\Delta H^0_{Mn\text{-}Co})^2 = (\Delta H^0_{Mn\text{-}Co})^2_{dip}$ and $\tilde{g}(\parallel [1,1,1]) = 6.6$, which was derived from the above μ^2_{eff} value by $\mu^2_{eff} = \tilde{g}^2\,\mu_B^2\,\tilde{J}(\tilde{J}+1)$ assuming $\tilde{J} = 1/2$, the pre-exponential factor a in (7) was calculated as $a = 1 \times 10^{-13}$ s from (22). In spite of a complete disregarding of the exchange contribution to the line broadening, the obtained a value shows a fairly good agreement with that (0.5×10^{-13} s) determined by the ^{35}Cl T_{1Q} analysis, suggesting the minor importance of the exchange contribution in this compound. From the a value, $\tau_s = 1 \times 10^{-11}$ s is calculated by (23). This value is appreciably shorter than that (9×10^{-11} s) from the ^{35}Cl T_{1Q} analysis. In the case of the ESR experiments of impurity Mn^{2+} ions, Mn-Co exchange interaction also affects the electron spin dynamics of Co^{2+} ions adjacent to the probe ions. This may be a possible reason why a shorter value of τ_s was obtained for Co^{2+} in the Mn^{2+} doped system.

[1] J. E. Wertz and J. R. Bolton, Electron Spin Resonance, Elementary Theory and Practical Applications, p. 332, Chapman and Hall, New York 1986.
[2] T. Mitsuma, J. Phys. Soc. Japan **17,** 128 (1962).
[3] G. C. Upreti and R. S. Saraswat, Magn. Reson. Rev. **7,** 215 (1982).
[4] R. Murugesan and S. Subramanian, J. Magn. Reson. **57,** 385 (1984).
[5] R. Hrabański, Chem. Phys. Lett. **123,** 182 (1986).
[6] M. Das and A. K. Pal, J. Phys. Chem. Solids **48,** 903 (1987).
[7] J. Lech, A. Ślęzak, and R. Hrabański, J. Phys. Chem. Solids **52,** 685 (1991).
[8] A. Birkeland and I. Svare, Phys. Scrip. **18,** 154 (1978).
[9] H. Rager, Z. Naturforsch. **36a,** 637 (1981).
[10] H. Rager, Z. Naturforsch. **39a,** 111 (1984).
[11] L. Pauling, Z. Kristallogr. **72,** 482 (1930), cited in: Crystal Data Determinative Tables, 3rd ed., vol. II: Inorganic Compounds, U.S. Department of Commerce, National Bureau of Standards, and the Joint Committee on Powder Diffraction Standards, USA 1973.
[12] A. Sasane, H. Shinohara, Y. Mori, Y. Kume, T. Asaji, and D. Nakamura, Z. Naturforsch. **42a,** 611 (1987).
[13] Gmelins Handbuch der Anorganischen Chemie, Pt(68), Teil C, Verlag Chemie, Berlin 1940.
[14] K. Horiuchi, R. Ikeda, and D. Nakamura, Ber. Bunsenges. Phys. Chem. **91,** 1351 (1987).
[15] A. Ishikawa, Ph.D. thesis, Nagoya University 1990.
[16] T. Asaji, L. S. Prabhumirashi, and D. Nakamura, Z. Naturforsch. **41a,** 1154 (1986).
[17] M. Mizuno, T. Asaji, and D. Nakamura, Z. Naturforsch. **44a,** 210 (1989).
[18] Y. Oyanagi and T. Nakagawa, SALS System Ver. 2.5 for statistical analysis with least-squares fitting, The University of Tokyo, Japan 1981.
[19] K. R. Jeffrey and R. L. Armstrong, Phys. Rev. **174,** 359 (1968).
[20] M. Mizuno, T. Asaji, and D. Nakamura, Z. Naturforsch. **45a,** 527 (1990).
[21] G. E. Pake and T. L. Estle, The Physical Principles of Electron Paramagnetic Resonance, 2nd ed., p. 205, Benjamin, Reading, Massachusetts 1973.
[22] M. Gerloch and P. N. Quested, J. Chem. Soc. (A) **1971,** 3729.
[23] G. M. Zverev and N. G. Petelina, Sov. Phys. JETP **15,** 820 (1962).
[24] M. H. L. Pryce, Proc. Roy. Soc. London **A 283,** 433 (1965).
[25] A. Abragam and B. Bleaney, Electron Paramagnetic Resonance of Transition Ions, p. 446, Dover, New York 1986, Clarendon Press, Oxford 1970.
[26] B. Bleaney and D. J. E. Ingram, Proc. Roy. Soc. London **A 205,** 336 (1951).
[27] Ref. [25], p. 142.
[28] Ref. [21], p. 101.
[29] Ref. [25], p. 55.
[30] C. P. Slichter, Principles of Magnetic Resonance, Third enlarged and updated ed., p. 80, Springer-Verlag, Berlin 1990.
[31] P. W. Anderson and P. R. Weiss, Rev. Mod. Phys. **25,** 269 (1953).
[32] M. Majumdar and S. K. Datta, J. Chem. Phys. **42,** 418 (1965).